A Review on Chipless RFID Tag Design

Invited Paper

Ali Hashemi[1], Amir Hossein Sarhaddi[2], and Hossein Emami[3]
1- Department of Electrical Engineering, Technical & Vocational University, Mohajer Center, Isfahan, Iran.
Email: aht1347@yahoo.com
2- Department of Electrical Engineering, Majlesi Branch, Islamic Azad University, Isfahan, Iran
Email: ah_sarhadi@yahoo.com
3-Young Researchers Club, Majlesi Branch, Islamic Azad University, Isfahan, Iran
Email: h.emami@iaumajlesi.ac.ir (Corresponding author)

ABSTRACT:
The demand for RFID tags has recently increased due to the development of the RFID. Over the past decade, great efforts have been devoted to the design of RFID tags without chip inside. The concept of chipless RFID tags appears to be a promising solution for low cost item tagging because the cost of active RFID tag depends mainly on the chip used in them. This paper presents the progress of the chipless RFID tag and introduces major studies in this filed. Advantages and disadvantages of these methods are pointed out.

KEYWORDS: Chipless RFID tag, Frequency signature coding, Time domain RFID.

1. INTRODUCTION

Radio Frequency Identification (RFID) is a wireless system that uses radio frequency electromagnetic field to exchange data between tags attached to an object and the reader device which propagates integrator signals for identification and tracking applications. RFID tags which do not contain a silicon chip are called chipless tags. Different methods are reported in recent years for data encoding in chipless RFID tags. Generally, these methods can be classified in two categories: time domain and spectral (frequency) signature. The major studies on these methods and different applications for them are described in this paper.

2. TIME DOMAIN RFID TAGS

In this method integrator signal is sent toward tag from the reader. The tag sent echo pulses to the reader after a short time and with some time delays. This response is called backscattered signal. Usually computer software analyzed delayed backscattered pulses and informs Tag ID. Different technologies are used for development of Time domain RFID tags; Transmission line, TFT (Thin Film Transistor) RFIDs, Saw tags.

2.1. Transmission line

A transmission delay line based ID generation circuit for RFID tag is presented in [1]. Microstrip line is used as transmission line in this UHF band tag. As shown in Fig. 1 a short sinusoidal wave is sent into two microstirp branches, one, straight line and the other, longer meandered branches. The ends of the microstrip branches are either terminated with a resistor of value equal to Z_0 or with ports of similar impedance to avoid reflections. The signals in each of the branches get delayed by different time delays. Using isolators, the signal in the meandered branch is tapped at time delays equal to the discrete multiples of the width of the input signal. The tapped signals with different time delays are superimposed on to the straight branch to produce an output signal. The output signal can be interpreted as a combination of 1 s and 0 s (Fig. 2). Time delay (T_d) of microstrip line in Fig. 2 can be obtained from (1).

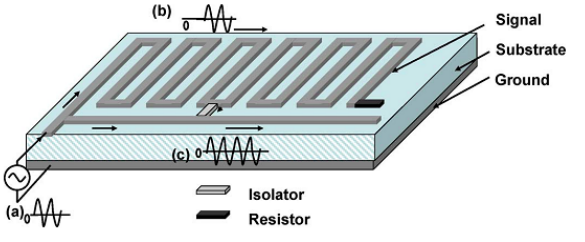

Fig. 1. Transmission delay line based ID generation circuit

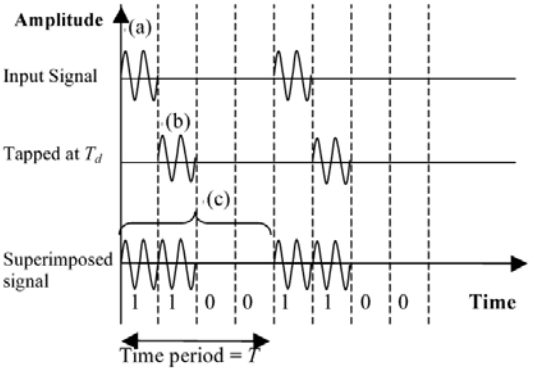

Fig. 2. Binary code generation of transmission line of Fig. 1

$$T_d = \sqrt{LC} \quad (1)$$

Although the microstrip delayed based tag can be printed on some objects but low capacity of coding is the main disadvantage of them. Only 4 bits of data has been successfully encoded using this tag.

Another printable tag which can encode higher bits has been proposed in [2]. An 8-bit tag with discontinuities, which were made by embedded passive components, has been presented. Impedance mismatched along microstrip line is used to reflect waves for encoding data. Both copper based planar capacitors and inject printing method can be used as passive planar capacitors with mismatched impedance in the structure but it is efficient to use inject printing to realize reconfiguration of the tags. The passive capacitors are pre-printed during tag fabrication and all are disconnected with the transmission line. When the tag comes to application, it will be reconfigured for different IDs by connecting the specific discontinuities to the transmission line. Fig. 3 shows an inject printing in a 4 bit tag. In fabricated tag, there are 8 capacitors along the transmission line. If the capacitor is connected with transmission line, there should be pulses in reflected wave, which stands "1"; if not, there is no pulse, which stands "0". An interrogation signal which consists of a train of Gaussian pulses with a 0.4ns pulse width and a period of 10ns is sent toward tag. In order to avoid overlap, the transmission line should be long enough to make the reflected wave appear at least after 0.4ns. The first reflected wave appears at 0.5ns, the second at 1ns, the third at 1.5ns and the last at 4ns as shown in Fig. 4. Every wave has the same pulse period 0.4ns, as the interrogation signal.

The proposed fully printable tag can be reconfigured easily by inkjet printers on fiber-based substrates such as paper. The transmission line and the 8 capacitors were prefabricated. What it is needed to do is to connect specific capacitors with transmission line by inkjet printing technology to accomplish the reconfiguration of the tags therefore an economical method for fully printable RFID tags has been introduce in this work however low coding capacity of them isn't sufficient for some applications.

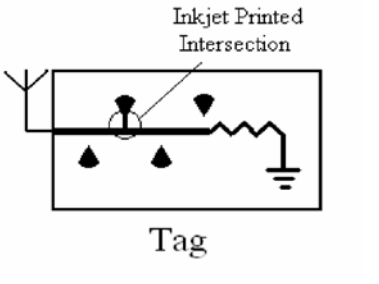

Fig. 3. Chipless RFID Tag based on impedance mismatched along microstrip line

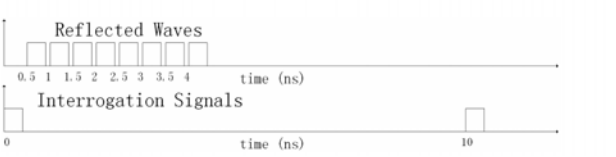

Fig. 4. Interrogation signal and reflected waves of RFID Tag based on impedance mismatched along microstrip line

2.2. Thin Film Transistor

Organic TFTs (Thin Film Transistor) are used in TFT RFID tags rather than conventional silicon chips. Although almost not many companies produce commercial TFT RFID tag but TFT is forecasted to be the main competitor for silicon chip-based RFID tags in next few years [3] because read-write functionality is achieved with this printable technology. Moreover they consume lower power than chip-based tags. Organic TFTs (Fig. 5) are operated between an "on" state, where the p-type semiconductor is accumulated of majority carriers at the interface with the dielectric, and an "off" state where the semiconductor film is progressively depleted of holes. Operation of an organic TFT tag is illustrated in [4]. As shown in Fig. 6 Capacitive coupling is chosen instead of the more common inductive coupling due to the lack of availability of a low resistance transparent inductor. The basic operation of this circuit is as follows; The power supply is located in the reader and through the capacitively coupled antenna transfers RF power to the RFID tag. The RFID tag contains a rectifier so that the incident RF power can be converted to DC power for use within the code generator. The code generator also modulates the rectifier, producing a coded signal that uses the RF power as a carrier wave. Once the RF wave and modulated code return to the reader, a demodulator extracts the code.

The code generator operation can be broken down into five main parts, a data array, synchronization block, power on reset block, ring oscillator, and rectifier/modulator block as shown in Fig. 7

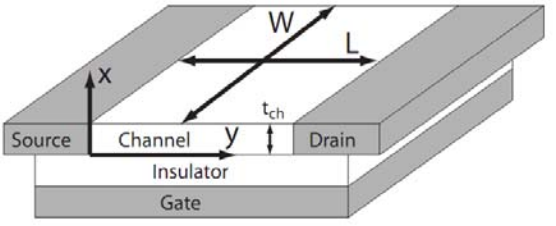

Fig. 5. Simple schematic TFT structure including the TFT dimensions of channel width, W, length, L, and thickness, T_{ch}

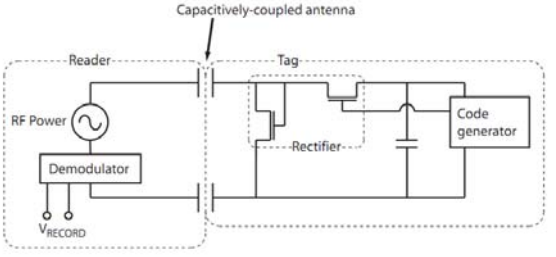

Fig. 6. Schematic of TFT RFID Tag with Capacitively-coupled antenna

The code generating data array is a grid of TFTs with hard coded data bits (i.e., 1's or 0's) placed on their drain contacts. The data bits are accessed by clock controlled shift registers for both the column and row indexing. Each shift register contains one SR latch (i.e., a set/reset flip-fop) for each row/column. The data array of Fig. 7 is a 16 bit array. Fig. 8 is the simulated output from the 16 bit array. The top plot shows the output of the row indexing shift register. The middle plot shows the output of the column indexing shift register. The column indexing is performed four times slower than the row indexing to allow for individual indexing of any single bit. The bottom plot is the final generated code output, showing the combination of the row and column indexing, as well as the hard-coded data bits. The synchronization block serves to synchronize the data from the 16 bit array to the RF carrier wave. The power on reset block serves to reset all the SR latches and data back to zero. The ring oscillator provides the clock signal for all signal processing. The rectifier/modulator block is the same rectifier that is used for RF-to-DC power conversion, as well as for inputting the 16 bit coded signal onto the RF carrier wave that is shown in Fig. 6.

2.2.1 Key Specification of TFT RFID tags

A. Operating Frequency

13.56 MHz is the desired frequency for item level tagging at medium distances. Higher frequencies, such as 900 MHz, are not ideal because they are affected by the material that the label is attached to, such as any metal or water that is inside the container. Lower frequencies, on the other hand, require significantly larger circuit components thereby making the device not only more bulky, but also more expensive to fabricate per unit. TFTC frequency is controlled primarily by channel length (source to drain), voltage and carrier mobility. To improve frequency beyond the current HF (13.56MHz) achieved by organics we need to print shorter channel length or improve carrier mobility in the semiconductor. Shorter channel length

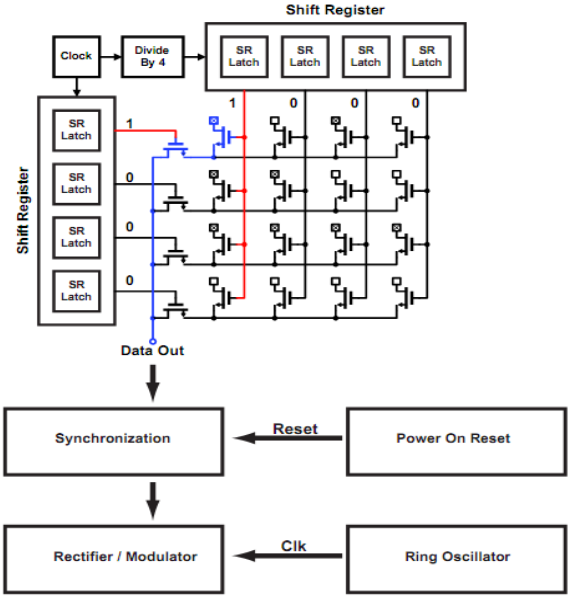

Fig. 7. Schematic of a 16 bit RFID tag code generator

Complicates fabrication. Moreover Low electron mobility limits the frequency of operation up to several MHz in current TFT RFID tags. The mobility that counts is not the basic physical parameter but the performance achieved in a particular construction and it does, to some extent, depend on that construction. However, it mainly depends on the chemistry of the material. The other alternative of using higher voltage is impracticable because of incompatibility with other devices, insulation and safety problems.

B. Operating Voltage

The current operating voltage of TFT is in the 10-20V range. In order to have long reading ranges, this high operating voltage will require power transmission above regulatory limits. Therefore the operating voltage should be within a 3-5V range.

C. Cost

The cost of each RFID tag is still higher than that of barcodes, whose cost is essentially the price of paper, but RFIDs will have many more savings down the line since they do not require any human intervention to operate. TFT is predicted to be one of the cheapest tags in the market until 2019. A lot of tracking processes can therefore be entirely automated, eliminating the

need to pay wages to a human being. TFT will be used in applications were cost is the key factor, not performance, since silicon RFIDs will likely remain dominant. Some cost-sensitive applications include individual tagging of consumer items for supply chain management (basically replacing the bar code), tagging for product authentication, smart cards for security, and tickets for events. Traditional Si RFIDs have seen only limited exposure to these applications because for wide spread adoption, the cost is currently too high.

The two fabrication processes that will work for the large-scale fabrication of organic RFIDs are vacuum deposition and solution printing. The fabrication process chosen needs to have a high yield and also low cost. Vacuum deposition will result in the highest mobility and purity, but unfortunately costs about the same as conventional silicon fabrication. It also has a low throughput for semiconductor. Furthermore, it also requires a shadow mask for patterning. Thus, vacuum deposition may be not as well suited for large-scale fabrication. Solution printing can be achieved easily using inkjet printing which is cheap, but has a very poor resolution of only about 30-40 μm. Another printing technique is simple spin coating which is extremely cheap, but requires photolithography and the associated masks to pattern the device. Other techniques include gravure printing and flexographic printing. A common solution is to combine many different printing techniques into one manufacturing process [5]. This strategy seems to offer the best cost vs. complexity trade off.

D. Read range, Coding capacity and Size

As mentioned just a few companies produce TFT RFIDs currently. Recently A German company (PolyIC) has manufactured this kind of tag named PolyID [6]. This product is an organic RFID that has a memory capacity of several bits and has been used in areas such as trademark protection, authenticity control, sorting functions, and logistics. It is said to be roll to roll printed using polythiophene as the semiconductor, and printed on a flexible polyester film. They are mounted on an antenna and have a read range of about 1 meter. Longer read range (up to 3m) is expected for newer TFT RFIDs in the future. In TFTs electromagnetic wave supplied by the reader is rectified to provide the tag power therefore the range is greatly reduced.

Coding capacity of current TFT RFID tags is up to 128 bits and physical size of the tag is about 2-10 cm^2. Tags with higher coding capacity (up to 1Kbit) and smaller size will be released in the future.

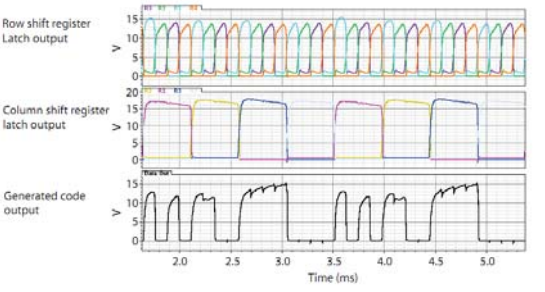

Fig. 8. Simulated output of a 16 bit RFID tag code generator.

2.3. Surface Acoustic Wave (SAW)

The basic operation of a SAW-based RFID system is shown in Fig. 9. In its simplest form, a single pulse of RF signal is sent from the reader antenna to the SAW tag. At the tag, the signal is received by the tag antenna which is connected to an Inter-Digital Transducer (IDT) on the SAW device. The SAW device is built on a bar of crystalline material such as lithium niobate which is piezoelectric. The received reader signal that appears on the IDT from the antenna is now converted to a nano-scale Surface Acoustic Wave (SAW) replica of the reader RF Signal. The wave travels down the length of the SAW device and is then partially reflected at wave reflectors that have been placed on the surface of the device. These reflected waves then travel back to the IDT where they are reconverted to an electrical signal by the reverse piezoelectric effect and are radiated by the tag antenna to be sent to the reader antenna. The information that is encoded on the device is contained in the precise location of the wave reflectors for a given tag code. Reference [7] describes a SAW based RFID system. This work has reviewed the Hazards of Electromagnetic Radiation to Ordnance (HERO) standards and calculation methods to evaluate the performance of a SAW Based RFID system. Further, this paper has shown that it is practical to build SAW Based RFID systems that simultaneously meet the most stringent HERO UNSAFE and HERO UNRELIABLE ORDNANCE requirements and provide excellent reading range performance.

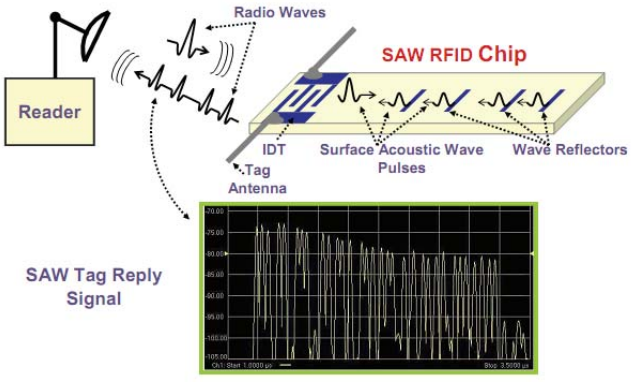

Fig. 9. System operation of SAW tag and its reply signal for a 128 bits tag

Saw tags advantages include; Long read range (up to 30 meter) with low power reader, reliable communication (because of using PM/PPM modulation), rapid read speed, isolation between integrator signal and its echoes (tag does not start sending reply until 1 microsecond after receiving integrator signal), High data capacity (up to 256), Reading of tagged items that have metal or liquid content and reliable reading under non-ideal conditions (e.g., wet tags, obscured tags, etc.). SAW tags are also preferred that they are resistant to gamma radiation and also low/high temperature. RFSAW © has manufactured commercial saw tags for automatically track, manage, and control objects, supply chains and location of staff and assets in hospitals. In addition this kind of tag has been used in Highway non-stop tolling in USA.

Although Saw technology is more cost-effective than semiconductor RFID chips but it is more expensive than many others chipless RFID tags because of using costly piezoelectric substrate. Moreover it isn't fully printable due to piezoelectric nature. It seems that saw tag isn't expected to grow much in RFID market in future in comparison to other chipless RFID tags due to their characteristic limitations.

3. FREQUENCY DOMAIN-BASED TAGS

Resonant structures are used in frequency-based tags to encode incoming waves from readers. These tags usually use multi resonator transmission line. In this method, Tag ID is generated from a predetermined presence or absence of a set of resonance peaks in frequency response S_{21}. The higher coding capacity can be achieved in frequency domain than time domain. Artificial inclusions and standard planar structures are used in this method for encoding. Some major researches in this field are mentioned below;

Microstrip dipoles are used in [8] as resonant structure (Fig. 10). The length and width for the 5-6 GHz dipoles are taken identical for all dipoles as 18mm and 2.6mm, respectively. The value of tuning capacitor is selected to fix the resonance frequencies. The gap capacitor is changed from 1pF to 5.6pF for each dipole to exhibit unique resonance frequency. Identical conductor pattern for dipoles ease fabrication process for this kind of simple RFID tag but it has problems with size and parasitic mutual coupling of dipoles.

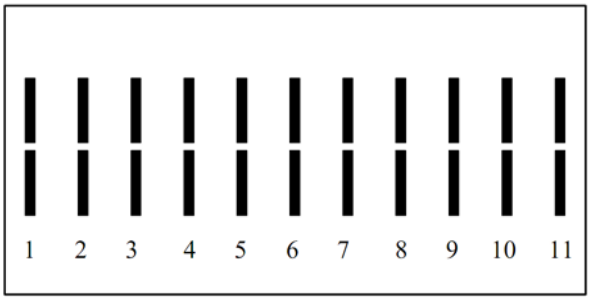

Fig. 10. Split dipoles RFID for 5.8 GHz bands

Another example of RFID tag in frequency domain is presented in [9] using Hilbert and Peano space filing curves. A space-filling curve orders points linearly to preserve the distance between two points in the 2D-space. This means that points which are close in space and represent similar data should be stored together in the linear sequence. Fig. 11 shows Hilbert and Peano curves. These curves are generally used in applications like; nearest neighbor search, indexing of higher-dimensional data (mapping multi-dimensional space to one dimension), storage and retrieval of multi-dimensional data in a database. An interesting property of a space-filling curve as an artificial magnetic inclusion is that as the higher iteration-orders of this curve are considered a long "line" can be compacted into a small "surface" area. From an electromagnetic point of view, such a curve may provide a structure that, although small in its footprint, it can be resonant at a wavelength much longer than its footprint. Such a "compact resonator" can be quite useful in various applications in radiation and scattering problems. Fig. 12 shows an example of 5 elements of a Peano curve. Each element consists of a Peano curve of order 2. Each element within the array are scaled to 95% of the physical size of the element to its left and by using this scaling factor, each element in the array is designed to resonate at a separate and particular frequency. When illuminated with a normally incident plane-wave excitation, these geometries gives rise to the scattering. Multiple peaks in the Radar Cross Section (RCS) are evident and each peak corresponds to the resonance of a different element within the array.

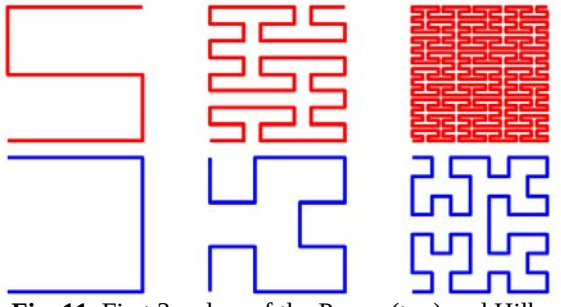

Fig. 11. First 3 orders of the Peano (top) and Hilbert (bottom) space-filling curves

Frequency dependency to polarization, elements mutual coupling, and significant layout modification to encode the desired data have complicated commercial manufacturing of space filling curves.

Refrence [10] presents a chipless RFID tag which is designed by stub-loaded resonator. The stub-loaded capacitor is shown in Fig 13. The outer line exhibits two resonance frequencies which $f_2 = 2 f_1$. The resonance frequency of open-ended stub can be tuned to placed at $f_r (f_1 < f_r < f_2)$ by designing the parameters l_s and Z_s which denotes respectively length and characteristic impedance of open-ended stub. l_s can be calculated by (2). ϑ_p is the propagation velocity in the

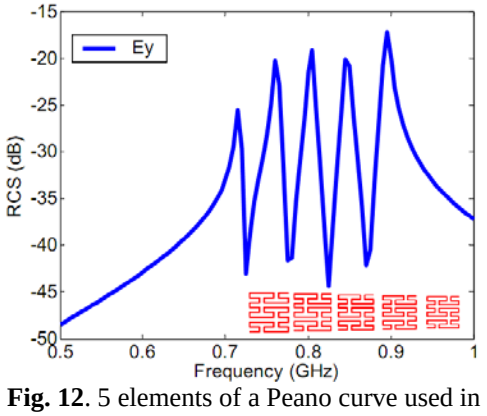

Fig. 12. 5 elements of a Peano curve used in an RFID tag and frequency signature of the tag

open-ended stub, and Z_1 defines characteristic impedance of outer line. Fig. 14 shows fabricated tag. Each resonator codes one bit in its first resonance, leading to two possible combinations (0, 1). When using stub-loaded resonators, each resonator can code information in the first and second resonances, and then three combinations can be obtained (00, 11, 10). The combination (01) cannot be obtained. Eight resonances can be observed: four fundamental resonances (the ones with lower frequency) and four second resonances generated with the stubs (the ones with higher frequency).

$$l_s \approx \frac{-Z_s \vartheta_p}{Z_1 \pi f_r} \tan\left(\frac{\pi f_r}{2 f_1}\right) \qquad (2)$$

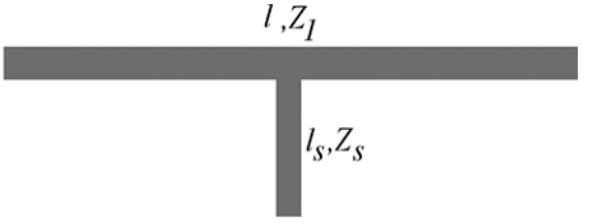

Fig. 13. Stub-loaded resonator

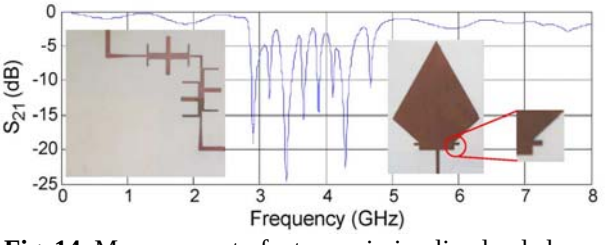

Fig. 14. Measurement of a transmission line loaded with four stub-loaded resonators. The tag is integrated with rhomboid antennas

Spilt ring resonators (SRR) and Spiral resonators (SR) inclusions are used in [11] and [12] as coding elements for printable chipless RFID applications. By varying the parameters of the SRR and the directions of the gaps in [11], resonance frequencies can be varied. Layout of the tag is shown in Fig. 15. If the parameters are varied, equivalent capacitances and inductances are changed and significantly affect the resonance frequency. The tag size is suitable for ID cards applications but data capacity of it is very low (only a 4 bits tag). In contrast, RFID tag which is proposed in [12] encodes large number of bits (up to 35 bits) but tag size increments with number of bits. This work presents a shorting method with laser etching technique in time of utilization of tag which ease fabrication process.

As mentioned above one of the main challenge in designing printable chipless RFID tags is to achieve higher data density in a fixed area. Two novel compact chipless RFID tags are presented in [13] and [14] which have considered this concern. Slot resonators on patches have been used in them. If a slot resonator is placed inside a metallic patch, it will give signature at its resonant frequency. If 'N' slots of different lengths are placed inside the metallic patch then it will give signatures at 'N' different frequencies. The asymmetric second order resonant frequency for this slot resonator is not excited due to symmetrical excitation. These frequency signatures are independent of each other and can be removed by just removing or shorting the slots. Moreover, if a slot is illuminated with an orthogonally polarized plane wave, no surface current will be

induced around the slot .This polarization property of the slot resonator is applied in [13] to double the encoding capacity using slots with two orthogonal polarities. As shown in Fig. 16, eight slots are placed in two upper patches (Slots aren't placed in one patch to reduced mutual coupling moreover, to obtain a measurable gap between frequency notches). Then similar sets to upper vertical patches are placed at bottom horizontally. The tag is excited by a dual-polarized transmitter antenna (Tx) and the frequency encoded backscattered signal from the tag is received by another dual-polarized receiver antenna (Rx). The V-polarized receiver (Vr) will receive the frequency encoded signal from the V-slots of the tag, since they show frequency response only to the V-polarized transmitted signal (Vt). Similarly the H-polarized receiver (Hr) will receive the frequency encoded signal from the H-slots, which respond only to the H-polarized transmitted signal (Ht). The bits can be removed simply by shorting the slots at their corner points which will take the resonant frequencies of the slots outside of the frequency band of interest (Fig. 17).

Reference [14] proposes a compact printable tag. which consists of a circular patch loaded with multiple slot ring resonators. An 8 bit tag was fabricated and due to its symmetric structure frequency signature at any orientation of the ring resonator with the reader antenna is the same. The tag and its principle of operation are shown in Fig. 18. Read range of this tag is almost 2

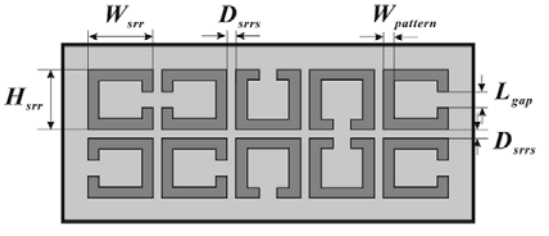

Fig. 15. Layout of the tag with defined parameters [11].

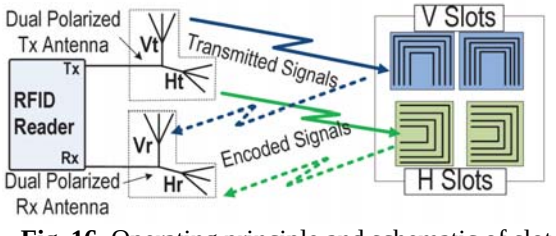

Fig. 16. Operating principle and schematic of slot-loaded dual-polarized chipless RFID Tag

meters. When a plane wave excites this slot ring resonator loaded patch, it shows a frequency selective behavior with peaks followed by deep notches at the resonant frequencies of the ring resonators. The number of bits can be increased by increasing the number of ring resonators within the patch. The logic state of a bit can be changed by removing the slot ring resonator which will remove the resonant frequency of the slot. The removal of notch frequency is denoted as logic '0' where the appearance of a notch is denoted as logic '1'. The proposed tag can be directly printed on the paper or plastic packets of the items, and also can be inserted inside ID cards. Fig. 19 shows some examples of simulated tags and their IDs. Removal of the slots to create bit 'o', causes shift in frequency response and it is a disadvantage for this work. The author has suggested overcoming these little shifts by signal processing methods at the reader side.

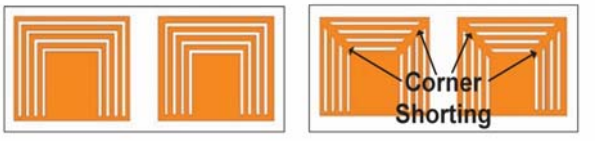

Fig. 17. Slot can be shorted to remove bits in slot-loaded dual-polarized chipless RFID tag . The left tag ID is 11111111 and the right tag has ID of 00000000.

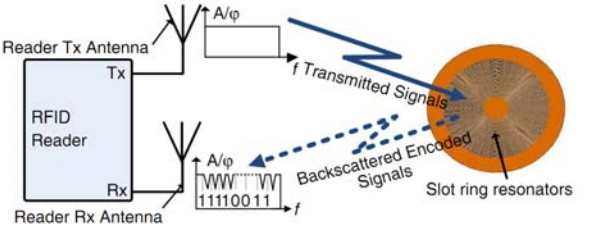

Fig. 18. Circular RFID tag loaded with multiple slot ring resonators and its operation.

4. CONCLUSION

It is predicted that the numbers of chipless tags sold globally will rise from 40 million 1.7% of the market in 2009 to 624 billion 88% in 2019 [3]. Many companies and universities are working on chipless RFID tag and new promising version of this technology has been introduced but it seems that none of them isn't the right candidate for barcode replacement yet and doesn't cover different applications demands as mentioned above in this paper. The dream for the future is a printable chipless RFID tag costing only a few cents that contains small layout size, long read range, high data capacity and high resistance to environmental conditions such as noise and temperature. Therefore more efforts should be spent on chipless RFID technologies to gather all above specifications in an RFID tag. Among different technologies it seems that organic TFTs have a promising future in the market of RFID. They are a good solution for different applications but they are currently very expensive and don't support long stable read range.

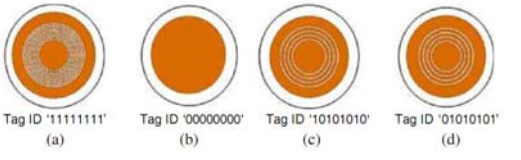

Fig. 19. Layout of the simulated tags with different IDs. (a) `11111111', (b) `00000000', (c) `10101010', and (d) `01010101'.

REFERENCES

[1] A. Chamarti and K.Varahramyan, **"Transmission delay line based ID generation circuit for RFID applications,"** *IEEE Trans. Microw. Wireless Compon. Lett*, vol. 16, pp. 588 – 590, Nov. 2006.

[2] L. Zheng, S. Rodriguez, L. Zahng and B. Shao, **"Design and implementation of a fully reconfigurable chipless RFID tag using inkjet printing technology,"** *in IEEE Int. Circuits Systs. Symp***.,** *Seattle, WA, 18-21 May 2008,* pp. 1524 – 1527.

[3] P. Harrop and R. Das **"Printed and chipless RFID forecasts, technologies & players 2009-2029,"** IDTechEx, 2009, pp. 2

[4] E. S. Sundholm**, "Amorphous oxide semiconductor thin-film transistor ring oscillators and material assessment,"** M.S. thesis, Elect. & Comput. Eng. Dept., Oregon State Univ., pp. 81-84, 2010.

[5] V. Subramanian, J. M. J. Frechet, P. C. Chang and D.C. Huang, **"Progress toward development of all-printed RFID tags: materials, processes, and devices,"** *Proc. Of IEEE*, Vol. 93, pp. 1330 – 1338, July 2005.

[6] http://www.polyic.com/products/polyidr.html

[7] P. R. Hartmann, **"A passive SAW based RFID system for use on ordnance,"** *in 2009 IEEE Int. Conf. on RFID*, pp. 291-297.

[8] I. Jalaly and I. D. Robertson, **"Capacitively-tuned split microstrip resonators for RFID barcodes,"** presented at the *European Microw. Conf*. Paris, France, 4-6 Oct. 2005

[9] J. McWay, A. Hoorfar, and N. Engheta, **"Theory and experiments on Peano and Hilbert curve RFID tags,"** presented at the *Int. SPIE. Symp. On Defense and Security,* April 2006.

[10] D. Girbau, J. Lorenzo, A. Lazaro, C. Ferrater and R. Villarino, **"Frequency-coded chipless RFID tag based on dual-band resonators,"** *IEEE Antennas Wireless Propag. Lett.*, Vol. 11, pp. 126-128, 2012.

[11] H. S. Jang, W. G. Lim, K. S. Oh, S. M. Moon and J. W. YU, **"Design of low-cost chipless system using printab chipless tag with electromagnetic code,"** *IEEE Trans. Microw. Wireless Compon. Lett***.** Vol. 20, pp. 640-642, Nov. 2010.

[12] S. Preradovic and N. C. Karmakar, **"Design of fully printable planar chipless RFID transponder with 35-bit data capacity,"** *in Proc. 2009 Eur.Microw. Conf.*, pp. 013–016.

[13] M. D. A. Islam and N. Karamkar, **"Design of a 16-bit ultra-low cost fully printable slot-loaded dual-polarized chipless RFID tag,"** *in Proc. 2011 Asia-Pacific Microw. Conf.* pp. 1482-1485.

[14] M. A. Islam, Y. Yap, N. Karmakar, and A. Azad **"Compact printable orientation independent chipless RFID tag"** *Progress in Electromagnetic Research C*, Vol. 33. pp. 55-66, 2012.